International Journal of Nanomedicine

Dovepress
open access to scientific and medical research

Open Access Full Text Article

ORIGINAL RESEARCH

Topical Nano-Vesicular Spanlastics of Celecoxib: Enhanced Anti-Inflammatory Effect and Down-Regulation of TNF-α, NF-κB and COX-2 in Complete Freund's Adjuvant-Induced Arthritis Model in Rats

This article was published in the following Dove Press journal:
International Journal of Nanomedicine

Eman Alaaeldin[1,2]
Heba A Abou-Taleb[3]
Soad A Mohamad[1]
Mahmoud Elrehany[4,5]
Shereen S Gaber[5]
Heba F Mansour[2]

[1]Department of Pharmaceutics, Faculty of Pharmacy, Deraya University, Minia, Egypt; [2]Department of Pharmaceutics, Faculty of Pharmacy, Minia University, Minia, Egypt; [3]Department of Pharmaceutics and Industrial Pharmacy, Nahda University (NUB), Beni-Suef, Egypt; [4]Department of Biochemistry, Faculty of Pharmacy, Deraya University, Minia, Egypt; [5]Department of Biochemistry, Faculty of Medicine, Minia University, Minia, Egypt

Correspondence: Eman Alaaeldin
Department of Pharmaceutics, Faculty of Pharmacy, Minia University, P.O. Box: 61111, Minia, Egypt
Email Eman_alaa_eldin@yahoo.com

Background: Rheumatoid arthritis (RA) is an autoimmune disease that underlies chronic inflammation of the synovial membrane. Non-steroidal anti-inflammatory drugs (NSAIDs) are commonly used to treat RA. However, a long list of adverse events associated with long-term treatment regimens with NSAIDs negatively influences patient compliance and therapeutic outcomes.

Aim: The aim of this work was to achieve site-specific delivery of celecoxib-loaded spanlastic nano-vesicle-based delivery system to the inflamed joints, avoiding systemic administration of large doses.

Methodology: To develop spanlastic nanovesicles for transdermal delivery of celecoxib, modified injection method was adopted using Tween 80 or Brij as edge activators. Entrapment efficiency, vesicle size, ex vivo permeation, and morphology of the prepared nano-vesicles were characterized. Carbopol-based gels containing the selected formulations were prepared, and their clarity, pH, rheological performance, and ex vivo permeation were characterized. Celecoxib-loaded niosomes and noisome-containing gels were developed for comparison. The in vivo efficacy of the selected formulations was evaluated in a rat model of Freund's complete adjuvant-induced arthritis. Different inflammatory markers including TNF-α, NF-κB and COX-2 were assessed in paw tissue before and after treatment.

Results: The size and entrapment efficiency of the selected spanlastic nano-vesicle formulation were 112.5 ± 3.6 nm, and 83.6 ± 2.3%, respectively. This formulation has shown the highest transdermal flux and permeability coefficient compared to the other investigated formulations. The spanlastics-containing gel of celecoxib has shown transdermal flux of 6.9 ± 0.25 μg/cm^2/hr while the celecoxib niosomes-containing gel and unprocessed celecoxib-loaded gel have shown 5.2 ± 0.12 μg/cm^2/hr and 0.64 ± 0.09 μg/cm^2/hr, respectively. In the animal model of RA, the celecoxib-loaded spanlastics-containing gel significantly reduced edema circumference and significantly suppressed TNF-α, NF-κB and COX-2 levels compared to the niosomes-containing gel, the marketed diclofenac sodium gel, and unprocessed celecoxib-loaded gel.

Conclusion: The spanlastic nano-vesicle-containing gel represents a more efficient site-specific treatment for topical treatment of chronic inflammation like RA, compared to commercial and other conventional alternatives.

Keywords: nano-vesicles, spanlastics, celecoxib, niosomes, arthritis

submit your manuscript | www.dovepress.com
DovePress
http://doi.org/10.2147/IJN.S289828

Introduction

Rheumatoid arthritis (RA) is a chronic inflammatory autoimmune disease that affects joints and other tissues in about 1% of the worldwide population.[1] During the acute phase of the inflammatory response, cells of the immune system, stimulated by cytokines, migrate to the site of injury. Tumor necrosis factor alpha (TNF-α), a cytokine that primarily contributes to joint destruction during rheumatoid arthritis (RA), stimulates proliferation and differentiation of B lymphocytes, T lymphocytes and NK cells.[2] It also induces the production of other pro-inflammatory cytokines such as IL-1, IL-6. In addition, nuclear factor kappa-B (NFκB) is a transcription factor that regulates immune response during inflammation.[3] Cyclooxygenase-2 (COX-2) also participates in the inflammatory response, as it is the major enzyme in prostaglandin biosynthesis.[4,5] COX-2 plays an important role in articular cartilage disease and studies have reported that the expression of COX-2 facilitated the inflammatory cytokine-induced metabolic imbalance of cartilage proteoglycans, irreversibly promoting arthritis.[6,7] Arthritis is clinically manifested by stiffness of the joints, gradual loss of joint function, and chronic pain, which collectively leads to loss of self-sufficiency and disruption of life.[8] While there is no cure for arthritis, symptomatic management can improve the quality of life of patients. This includes pain control using non-steroidal anti-inflammatory drugs (NSAID).[9–12] Oral COX-2 inhibitors are currently recommended for the management of the pain accompanying arthritis. However, the long-term use of these drugs is associated with increased risk of gastrointestinal, cardiovascular, and renal adverse effects,[13] which explains the increased demand for a topical, site-specific, sustained-release delivery system loaded with NSAIDs, among other therapeutics, for the treatment of RA.[14–16]

The selective COX-2 inhibitor, celecoxib, is commonly used as an anti-arthritic drug, and it is available in the market as oral suspension, tablets or capsules. The drug is a very weak acid, with a PK_a value of 9.68, and it is highly lipophilic. It exhibits variable absorption profiles and delayed onset of action ranging from 3 to 4 hours after oral administration.[13] Moreover, celecoxib suffers hepatic first pass metabolism and rapid elimination from plasma.[17] The long-term use of celecoxib, as well as other COX-2 inhibitors, induces cardiotoxicity after oral administration. To improve therapeutic outcome of celecoxib and minimize the incidence of adverse events following its use, modified delivery approaches have been developed. In this regard, Shakeel et al reported the enhancement of celecoxib bioavailability when a transdermal nanoemulsion was used,[18] while Moghimipour et al reported the prospective application of celecoxib-loaded liposomes as a transdermal drug delivery system.[13] Dave et al achieved an improved anti-arthritic activity of celecoxib encapsulated into PEGylated liposomes.[19] Other nano-carriers of celecoxib showed improved cytotoxic,[20] anti-arthritic effect,[10] anti-inflammatory effect[21] and pain management properties.[22]

Spanlastics or modified niosomes are novel flexible-walled nano-vesicular systems that differ from common niosomes in that they contain only non-ionic surfactant, usually Spans, in addition to an edge activator. The surfactant molecules are arranged in a bilayer membrane assembly that encloses the active agent.[23] Inclusion of the edge activator induces destabilization of the bilayer membrane of the vesicular system by lowering the interfacial tension. Membrane destabilization imparts high elasticity and deformability to the vesicular system.[24] Due to the ultra-deformability of spanlastics, they possess the ability to squeeze themselves throughout the intracellular spaces of the stratum corneum and the skin layers that follow, passing into the target dermal tissues and thus, enhancing transdermal drug penetration.[25] Spanlastics maintain acceptable stability compared to other dosage forms like liposomes. They are non-irritant compared to other dosage forms that contain cationic surfactants, and they provide enhanced delivery due to their highly elastic deformable nature. For example, spanlastics have been reported to enhance the transdermal delivery of fluvastatin sodium[16] and haloperidol.[23]

The objective of the present work is to develop a spanlastic nano-vesicular-based delivery system to improve the topical permeation and minimize the adverse events of celecoxib. The severity of inflammation and the differential expression of TNF-α, NF-κB and COX-2 in a Freund's complete adjuvant-induced arthritis model in rats following the treatment of RA rats with the spanlastic nano-vesicle gels or other treatments were assessed and compared.

Materials and Methods

Materials

Celecoxib was a kind gift from Amoun Pharmaceutical Co (Cairo, Egypt). Cholesterol, Span 60, Tween 80 and Brij

35 were purchased from Sigma-Aldrich (St. Louis, MO). Caroxyfluorescein (fluorescent marker for vesicles) was purchased from Acros Organics (Geel, Belgium). Other chemicals and solvents used in the study were of analytical grade and purchased from El-Nasr Pharmaceutical Company (Cairo, Egypt).

Methods

Preparation of Celecoxib-Loaded Spanlastics and Niosomes

Spanlastics (SP) were prepared using the spraying technique/modified injection method reported previously.[26] Briefly, as shown in Table 1, the specified amounts of Span 60, Tween 80 or Brij 35 (edge activator) and celecoxib (5 mg) were dissolved in 2 mL absolute ethanol to prepare the organic phase. The resultant solution was loaded into a modified spraying apparatus. The aqueous phase was prepared by dissolving sucrose in 3 mL distilled water to prepare 9% w/v sucrose solution. The organic solution was sprayed onto the surface of the aqueous solution (200 µL per five seconds) in a closed system heated to 60º C and stirred at 1500 rpm. Spanlastics were then spontaneously formed upon removing the excess ethanol by evaporation via stirring at 1500 rpm for 20 minutes at 60°C. The obtained spanlastic suspension was kept overnight at 4° C to allow annealing of the formed bilayer. The resultant formulation was kept in the refrigerator pending further investigations.

Niosomes (N) were prepared using the spraying technique. Briefly, cholesterol, Span 60 and celecoxib were dissolved in ethanol (organic phase) which was sprayed onto the surface of the aqueous phase. Same procedures used to prepare spanlastics were also adopted herein to prepare niosomes.

Physicochemical Characterization of Celecoxib-Loaded Spanlastics and Niosomes

Entrapment Efficiency (EE%)

Free unencapsulated celecoxib was removed from the celecoxib-loaded spanlastics or niosomes by centrifugation (25,000 rpm for 60 minutes at 4°C). The separated nanovesicles were washed by re-suspension in methanol and centrifugation.[13,27] The washing step was repeated twice to insure complete removal of the free drug.[28] We have not reported any adverse influence of the centrifugation process on the vesicle integrity.[24] After each centrifugation step, the supernatant was collected, and the celecoxib content in it was measured by UV-Vis spectrophotometry at 253 nm[29] using an UV-Vis spectrophotometer (Shimadzu-50-02, Kyoto, Japan). The amount of celecoxib entrapped was determined by subtracting the amount of free drug from the total celecoxib included in the formulation.[30] The entrapment efficiency (EE %) was then calculated using the following equation:

$$EE\% = \frac{amount\ drug\ entrapped}{total\ drug\ amount} \times 100^{27}$$

Table 1 Molar Ratios of Components of the Prepared Spanlastics and Niosomes

	Span 60	Tween 80	Brij 35	Cholesterol
Sp1	1	–	1	–
Sp2	4	1	–	–
N1	4	–	–	1
N2	1	–	–	1

Vesicle Size, Size Distribution and Zeta Potential

Vesicle size and polydispersity index of the prepared spanlastics and niosomes were investigated in triplicate using Malvern Zetasizer Nano (Malvern Instruments, Malvern, UK) following proper dilution with purified deionized water at 25°C, as previously reported.[31]

Zeta potential of the prepared formulations was determined using Malvern mastersizer (3000E Malvern Instruments, UK) after proper dilution with Millipore water. The average zeta potential of three replicates was determined.[32]

Ex vivo Skin Permeation of Celecoxib-Loaded Spanlastics and Niosomes

All animal experiments and protocols mentioned herein were performed according to the guidelines for the Care and Use of Laboratory Animals of the National Institutes of Health (NIH 1985) and were reviewed and approved by the Pharmacy Research Ethics Committee (PREC) of Minia University (approval number 61/2019). Female rats were provided water and food ad libitum, exposed to 12-hour cycle of light and darkness, and they were left to acclimatize for 1 week before the experiments started. The hair of the abdominal skin was carefully removed by shaving. Twenty four hours later, mice were euthanized by cervical dislocation and their abdominal skin was collected. The skin fat was removed using isopropyl alcohol and a surgical scalpel. The skin was divided by scissors into pieces of proper size that were stored at −80 C pending further experiment. Within two weeks of collection, the excised shaved abdominal skin of female mice was thawed and used to study the ex vivo permeation of celecoxib from the prepared nanovesicles.[15]

Before the experiment, the frozen skin was soaked for one hour in sodium chloride solution (0.9% w/v). The skin was fixed on a modified Franz cell with a sample compartment that holds up to 50 mL of receptor medium. The skin was fixed in such a way that the stratum corneum faces the donor side (sample compartment), while the deeper skin layers face the receptor medium side (reservoir compartment). Twenty-five mL of citrate-phosphate buffer solution (pH 5.5) containing 0.5% w/v tween 80, used to maintain sink condition,[33,34] was used as a receptor medium.[15] One hundred µL of the prepared nano-vesicles were accurately added to the sample compartment. The whole unit was shaken at 50 rpm in a thermostatic shaker adjusted at 37 ± 0.5°C. Two mL samples were removed at predetermined time intervals for up to 6 hours. The samples were analysed spectrophotometrically by measuring the absorbance at 253 nm to determine the mean cumulative amount celecoxib diffused. This experiment was carried out in triplicate and the mean values were recorded.[35] Unencapsulated celecoxib suspension was used as a control. This suspension was prepared by dissolving celecoxib in the least amount of absolute ethanol followed by the addition of distilled water to reach celecoxib concentration equivalent to that of the studied formulations.

The ex vivo permeation kinetics of the studied nano-vesicles were investigated by fitting the permeation data to different mathematical models, including zero order, first order, and Higuchi diffusion models, as follows:

Zero-order: $R = K_0\ t$

First-order: $R = 1 - e^{-k1}\ t$

Higuchi diffusion model: $Q = K_H\ t^{1/2}$

where R or Q is the fraction of drug permeated at time t, while K, or K_H is the rate constant corresponding to each model.

Transmission Electron Microscopy (TEM)

A transmission electron microscope (JEM-1400, Jeol, Tokyo, Japan) operated at 80 kV, was utilized to visualize the morphology of the selected celecoxib-loaded spanlastics and niosomes. One droplet of the vesicular suspension was added on the top of carbon-coated copper grid. The grid was left to dry at ambient temperature before the examination.[26,36]

Preparation of Carbopol Gel of the Selected Celecoxib-Loaded Spanlastics and Niosomes

Carbopol 934 was used to prepare gel of the selected celecoxib-loaded spanlastics and niosomes. The gel was prepared by dissolving Carbopol 934 (1% w/v), propylene glycol (1% w/v, as penetration enhancer), glycerol (3%w/v, as plasticiser) in an appropriate amount of deionized water. The resultant mixture was stirred for 2 hours to ensure complete dissolution of the ingredients and homogeneity of the gel.[37] Appropriate amounts of celecoxib suspension, celecoxib-loaded spanlastics (SP2) or celecoxib-loaded niosomes (N2) were added to the mixture mentioned above and the mixture was then stirred for 30 minutes to achieve uniform dispersion. Two drops (about 120 µL) of triethanolamine were then added while stirring to neutralize Carbopol and induce the formation of the gel. The pH of the resultant gel was adjusted to 5.5 and the gel was kept at room temperature for 24 hours before further investigations.[38]

Characterization of the Selected Nanovesicles-Loaded Gels

The prepared gels were examined for clarity against white and black backgrounds. The pH of the prepared gels was measured (Mettler Toledo, Switzerland). Viscosity and rheological profiles were also determined using Brookfield DV-III viscometer (Stoughton, MA) equipped with spindle 94 that was rotated at a variable speed ranging from 1 to 50 rpm. The study conditions and temperature (37±1° C) were kept constant for the three gel preparations.[37] The viscosities were recorded at different shearing stress rates and plotted against these rates to obtain the corresponding rheological profiles.

Ex vivo Skin Permeation of the Selected Nanovesicles-Loaded Gels

Ex vivo permeation of the prepared gels was investigated through excised rat skin using the same procedures mentioned earlier for celecoxib-loaded spanlastics and niosomes. Permeation data were fitted to different mathematical models as mentioned above.[15]

In vivo Animal Study

In vivo evaluation of the selected celecoxib-loaded spanlastics and niosomes was conducted in a Freund's complete adjuvant-induced arthritis model in rats. All animal experiments and protocols mentioned herein were reviewed and approved by the Pharmacy Research Ethics Committee (PREC) of Minia University (approval number 61/2019).

Animal Conditions

Thirty male Wistar rats weighing 250–300 g (12–14 months old), were used in the study. The rats were maintained in propylene cages and were exposed to 12-hours

light/darkness cycle, at a temperature of 23 ± 1°C. Regular rat chow and tap water were provided to the rats ad libitum.

Induction of Arthritis

Before starting the study, the behaviour of all rats enrolled in the study was evaluated, and the right paw measurements of these rats were taken using digital calipers. Twenty-five animals were anesthetised via intraperitoneal (IP) injection of ketamine chloride (40 mg/kg). After that, 0.1 mL of Freund's Complete adjuvant (complete fraction of Mycobacterium butyricum suspended in mineral oil; Sigma, St Louis, MO, USA) was injected into the sub-plantar tissue of the right posterior paws of the rats as reported previously.[39] Animals were inspected on daily basis, by measuring the dimensions of the injected paws and observing the animal's general conditions and behaviors. Arthritis was developed in all injected rats within 10 days, in the form of the development of distinct localized edema (swelling).

Chronic Treatment with Celecoxib Formulations

Eighteen days following the induction of arthritis, rats were randomly divided into six groups.(n=5/group) Group I rats (no arthritis, negative control) were injected with 100 µL of 0.9% saline, group II rats (arthritis, vehicle control) were treated topically with the blank gel base, group III rats (arthritis, positive control) were treated topically with the marketed diclofenac sodium gel (Olfen® Gel, MUP, Egypt) at a dose of 4.5 mg/kg,[30] group IV arthritic rats were treated topically with celecoxib gel (1.55 mg celecoxib/kg), group V arthritic rats were treated topically with celecoxib spanlastic-containing gel (1.55 mg celecoxib/kg),[10] and group VI arthritic rats were treated topically with celecoxib niosome-containing gel (1.55 mg celecoxib/kg). The treatment formulations were applied twice daily. Measurements of edema were recorded on the 19th, 21st, 23rd, 25th, and 30th after the injection of the Freund's complete adjuvant. The data collected were represented as mean ± SD (n = 5). The percentage inhibition of edema was calculated using the following equation:

$$\%\ \text{Reduction of edema} = \frac{\text{C Freund's adjuvant} - \text{C formulation}}{\text{C Freund's adjuvant.}} \quad 15$$

where C is the circumference of the paw either after injection with Freund's adjuvant (C Freund's adjuvant) or after treatment (C formulation).

Total RNA Extraction from Rat Paw Tissue

Approximately 100 mg of the rat paw tissue was homogenized in 1 mL Trizol solution (Amresco, Solon, OH, USA) using an ultrasonic homogenizer (Sonics-Vibracell, Sonics& Materials Inc., Newtown, CT, USA). Total RNA was extracted from the tissue using trizol RNA extraction reagent (Amresco, Solon, OH, USA) according to the manufacturer's instructions. The total RNA concentration was determined spectrophotometrically at 260 nm. The purity was calculated according to the ratio A260/A280 per manufacturer's instructions. Samples with purity ≥ 1.7 were used for qRT-PCR using GAPDH (Glyceraldehyde-3-phosphate dehydrogenase) as a reference housekeeping gene for determination of the relative expression of TNFα, NFκB and COX-2.[40]

Real-Time qRT-PCR

cDNA synthesis was accomplished for equal quantities of total RNA in all samples using the RevertAid H Minus First Strand cDNA Synthesis kit (K1632, Thermo Scientific Fermentas GmbH, St. Leon-Ro, Germany). Real-time polymerase chain reaction (PCR) was carried out using single-stranded cDNAs, and Maxima SYBR Green qPCR Master Mix (2X) (Thermo Scientific Fermentas GmbH, St. Leon-Ro, Germany) with the help of StepOne (PCR) Detection System (Applied Biosystems, Life Technologies GmbH, Frankfurt,

Table 2 Forward and Reverse Primer Sequences of Studied Markers

Marker	Sequence	Accession No.	Amplicon Size (bp)
TNF –α	F-5′-AGGACACCATGAGCACGGAA-3′ R-5′-GGGCCATGGAACTGATGAGA-3’	NM_012675.3	234
NF-kB	F-5′-GCAACTCTGTCCTGCACCTA-3′ R-5′-CTGCTCCTGAGCGTTGACTT –3’	NM_001276711.1203	203
COX-2	F-5′-GCATTCTTTGCCCAGCACTT-3′ R-5′-GTCTTTGACTGTGGGAGGAT-3’	NM_017232.3	210
GAPDH	F-5′-TCTCTGCTCCTCCCTGTTCT-3′ R-5′-CTTGCCGTGGGTAGAGTCAT-3’	NM_017008.4	229

Germany). The used set of primers is mentioned in Table 2. Real-time polymerase chain reaction (qRT-PCR) was carried out using 20 µL of RealMOD Green qRT-PCR Mix kit (iNtRON biotechnology) with 0.02 µg RNA per reaction containing 10 Pmol of specific primers, for 30 cycles of 95° C for 10 sec, and 60°C for 1 min. Comparative Ct (threshold cycle) method was used to determine the relative amounts of the products. The relative expression was calculated using the formula 2 (-ΔΔCt).[41] They were scaled relative to controls where control samples were set at a value of 1.

Statistical Analysis

All studies were carried out in triplicate and the average value ± SD was calculated. Analysis of variance (Welch ANOVA) with a 95% confidence interval was employed for statistical analysis for the data (XLSTAT software, Addinsoft).

Results

Physicochemical Characterization of Celecoxib-Loaded Spanlastics and Niosomes

Entrapment Efficiency (EE%)

The EE% of the prepared spanlastics and niosomes was investigated to determine the amount of celecoxib loaded in these nanovesicles and the results are displayed in Table 3. The entrapment efficiency of SP2 (83.6±2.3%) was significantly higher (P< 0.05) than that of SP1 (68.3 ±3.4%). The entrapment of N2 (76.4±2.4%) was higher than that of N1 (65.3±5.4) (P< 0.05).

Vesicle Size, Size Distribution and Zeta Potential

The vesicle size and polydispersity index (PDI) of the prepared spanlastics and niosomes are shown in Table 3. SP2 and N2 exhibited vesicular sizes of 112.5± 3.6 and 165.3± 5.3 nm, respectively. They are significantly smaller than those of SP1 and N1 (154± 3.2 and 326.5± 12.6 nm, respectively) (P< 0.0001). PDI values of the prepared nanovesicles ranged between 0.126 and 0.321. Zeta potential values ranged between - 13.6 to −17.5.

Table 3 Entrapment Efficiency, Vesicle Size, Polydispersity Index (PDI) and Zeta Potential of the Prepared Spanlastics and Niosomes

	EE%	Vesicle Size (nm)	PDI	Zeta Potential
Sp1	68.3±3.4	154±3.2	0.321±0.12	− 13.6±1.5
Sp2	83.6±2.3*	112.5±3.6***	0.126±0.09	−17.5±3.4
N1	65.3±5.4	326.5±12.6	0.213±0.034	−14.3±2.5
N2	76.4±2.4	165.3±5.3***	0.245±0.021	−16.3±1.2

Note: *p<0.05, ***p<0.005.

Ex vivo Skin Permeation

Ex vivo permeation was investigated to predict the in vivo performance of the prepared nanovesicles upon topical application for transdermal delivery. Ex vivo skin permeation profiles of celecoxib-loaded spanlastics and niosomes through excised rat skin are displayed in Figure 1. It is obvious that SP2 and N2 exhibited significantly higher skin permeation rates than those of SP1 and N1, respectively ($p < 0.05$). All the prepared nanovesicles demonstrated significantly higher skin permeation than that of celecoxib suspension. The percentage of celecoxib permeated through the excised rat skin over the first hour was 41.3 ± 1.9% and 25.7 ± 2.1% from SP2 and SP1, respectively. Furthermore, N2 and N1 permeated 30.2 ± 1.5, and 18.5 ± 1.5, respectively. On the other hand, celecoxib suspension permeated only 5.3 ± 0.68%. At the end of the permeation study (6 hours), the percentages of celecoxib permeated were 85.2 ± 3.4%, 62.3 ± 3.6%, 74.2 ± 3.0%, 43.2 ± 3.0% and 12 ± 4.2% for SP2, SP1, N2, N1 and celecoxib suspension, respectively. Additionally, SP2 had the highest transdermal flux and permeability coefficient compared to all other studied formulations (Table 4). Table 5 displays the correlation coefficient (r^2) of permeation of the studied nanovesicles following fitting to different mathematical models mentioned in the experimental section. It is obvious that Higuchi's diffusion was the best fitting model.

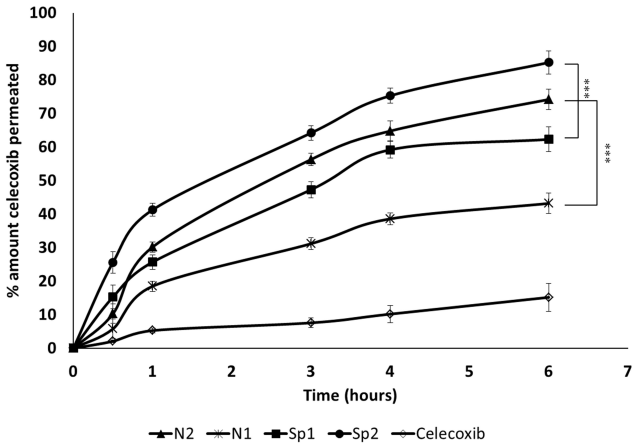

Figure 1 Ex vivo skin permeation of SP1, SP2, N1, N2 and celecoxib suspension. ***p<0.005.

Table 4 Transdermal Flux from ex vivo Permeation Study of the Selected Formulations

Formulation	Transdermal Flux (Jss) (μg/cm^2/hr)	Permeability Coefficient (cm h^{-1}) ×10^{-3}
N2	7.3±0.12***	10.9±0.15***
N1	4.2±0.31	5.4±0.24
Sp1	6.02±0.42	10.2±0.2
Sp2	7.6±0.24***	11.4±0.13***
Celecoxib suspension	1.4 ±0.08	3.5±0.4
N2 gel	5.2±0.12***	9.2±0.26***
Sp2 gel	6.9±0.25***	10.5±0.32***
Celecoxib gel	0.64±0.09	2.9±0.6

Note: ***p<0.005.

Table 5 Mathematical Modeling of Permeation Kinetics

Formulation	R^2		
	Zero	First	Higuchi
N2	0.821	0.832	0.971
N1	0.742	0.753	0.986
Sp1	0.865	0.812	0.984
Sp2	0.862	0.732	0.991
Celecoxib suspension	0.856	0.964	0.823
N2 gel	0.745	0.856	0.985
Sp2 gel	0.823	0.821	0.993
Celecoxib gel	0.863	0.832	0.961

Morphology of the Selected Nanovesicles

Based on the results of entrapment efficiency, vesicle size and ex vivo study, SP2 and N2 were selected for investigation of morphology and further studies. TEM images of SP2 and N2 are displayed in Figure 2. Both spanlastics and niosomes demonstrated uniform spherical shapes with smooth surfaces, good dispersion and no aggregations.

Characterization of the Selected Nanovesicles-Containing Gel

Visual inspection revealed that SP2 and N2-containing Carbopol gels were transparent, clear, homogeneous and free from any clogs. The pH of the gels was around 6.8 ± 0.2. Viscosity was diminished upon increasing the shearing rate from 1 to 50 rpm (Figure 3). Ex vivo skin permeation profiles of the selected nanovesicles-containing gels through excised rat skin and that of celecoxib gel are displayed in Figure 4. It is obvious that SP2-containing gel exhibited a significantly higher skin permeation than that of N2 and celecoxib loaded gels ($p < 0.05$). Transdermal flux and permeability coefficient of the studied gels are displayed in Table 4. SP2-containing gel showed flux of 6.9±0.25 μg/cm^2/hr while N2-containing gel and celecoxib-loaded gels displayed 5.2±0.12 and 0.64 ±0.09 μg/cm^2/hr respectively. Table 5 displays the correlation coefficient (r^2) for the studied gels. It is obvious that Higuchi's diffusion was the best fitting model.

Anti-Inflammatory Effect in Freund's Complete Adjuvant-Induced Arthritis

The percentage of edema reduction was determined in treated groups with respect to the control group (Table 6). Results show that at day 30 of induction of arthritis, after 7 days of treatment, the % of reduction of edema in the groups treated with diclofenac sodium gel (Olfen®) and celecoxib gel were comparable (42.13 ± 2.2% and 40.25 ± 4.3%, respectively). The use of celecoxib-loaded niosomes or spanlastic gels (N2, SP2) significantly increased the edema reduction percentage to 64.1 ± 3.5% and 73.45 ± 2.6%, respectively ($p< 0.0001$). Interestingly, spanlastic gel of celecoxib (SP2) showed significantly higher edema reduction percentage than that of the niosomal gel (N2) ($P <0.005$).

Relative mRNA Expression

Relative mRNA expression of TNF-α, NFKB and COX-2 was significantly increased in group II (arthritis, positive control) after induction of inflammation compared to group I (no arthritis, negative control) ($p \leq 0.001$). Up-regulation of the 3 markers indicates that inflammation was successfully induced. Table 7 displays the mean values of the relative expression of TNFα, NF-kB and COX-2 in groups III, IV, V and VI. Table 7 and Figure 5 reveal that the relative expression significantly decreased ($P \leq 0.005$) in all the treated groups regardless of the type of the formulation. This indicated that all the markers were down-regulated after treatment, which illustrates alleviation of the induced-inflammation by the applied treatments. SP2 and NS displayed significantly better reduction of expression of the three inflammatory markers ($P \leq 0.005$) compared to other groups. Noticeably, the spanlastic gel formulation showed significantly lower expression of the 3 markers compared to niosomal gel ($P \leq 0.05$).

Discussion

Optimization of a nanosized drug delivery system could have a great potential in the enhanced therapeutic effect of the

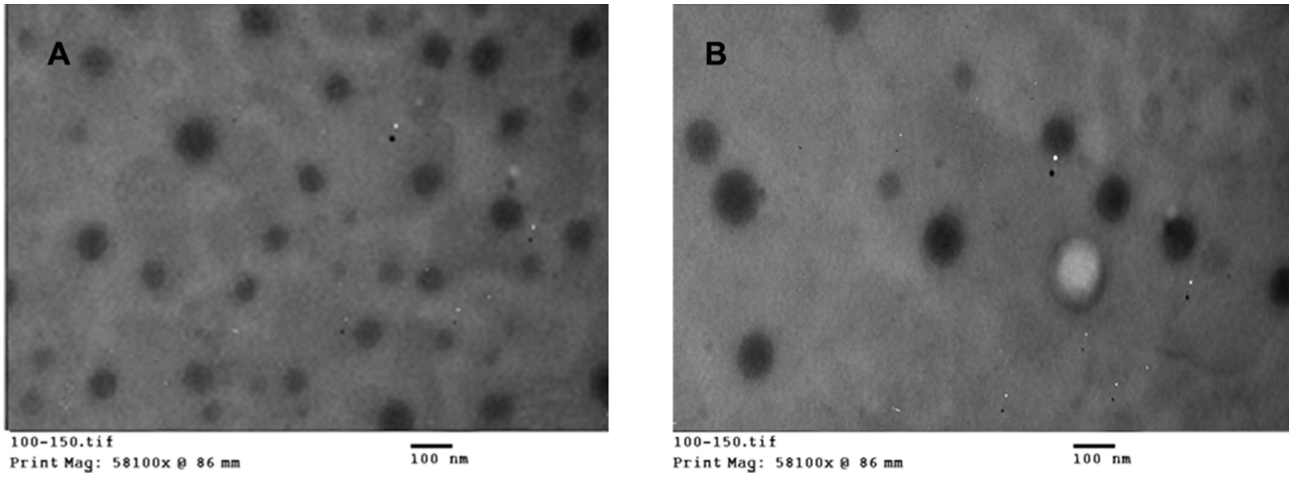

Figure 2 Transmission electron microscope images of (**A**) SP2, (**B**) N2.

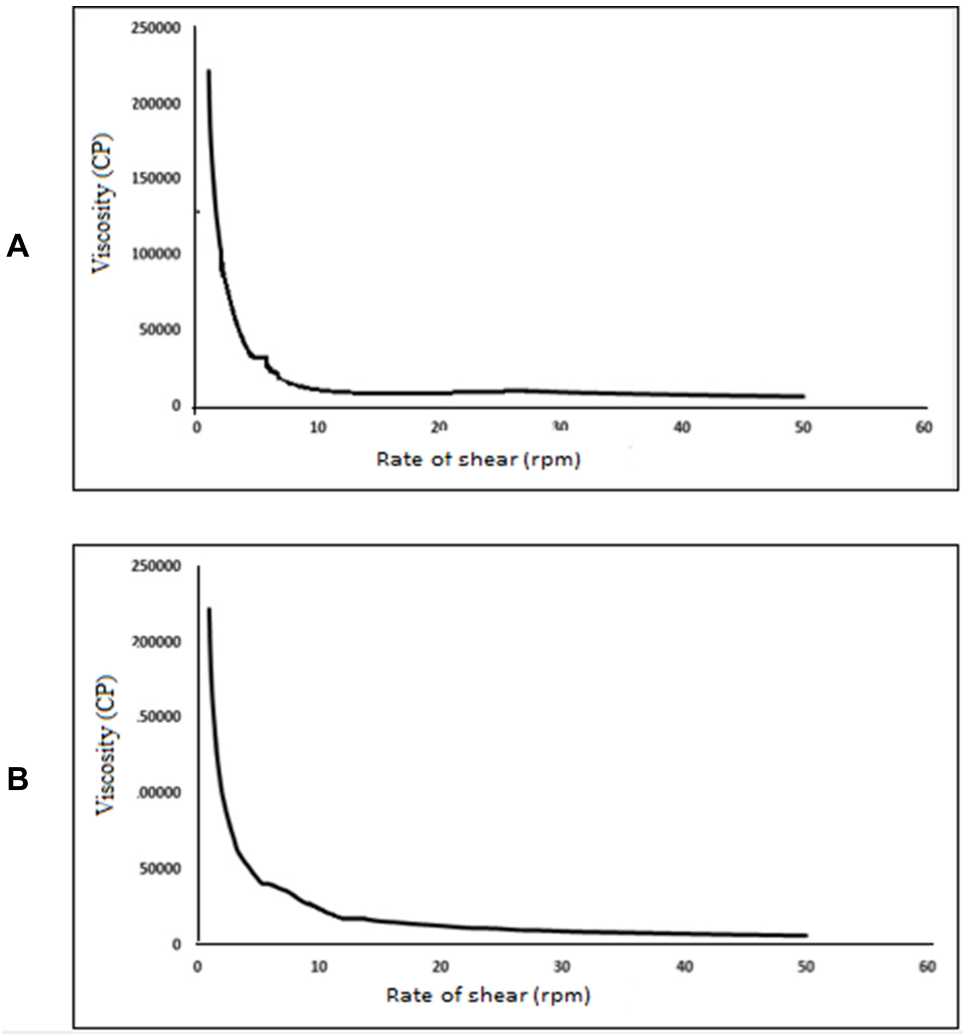

Figure 3 Rheology of (**A**) N2 gel, (**B**) SP2 gel.

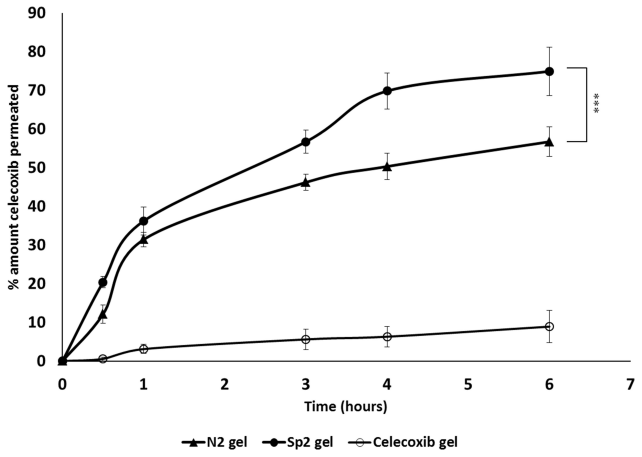

Figure 4 Ex vivo permeation of SP2 gel, N2 gel and celecoxib gel. ***p<0.005.

entrapped cargo.[42,43] In this study, we aimed to reduce the vesicular size and enhance the EE% and the skin permeation of celecoxib within two different nanosized formulations (spanlastics and niosomes). The use of Tween 80 (an edge activator with HLB value of 15) to prepare SP2 resulted in higher EE% compared to Brij (HLB =16.9) which was used in SP1. Previous studies reported that EE% increased as the HLB of the edge activator decrease.[16,44] Moreover, increasing the concentration of the Span 60 in SP2 lodged more drug within its hydrophobic vicinity,[45] and promoted the formation of multi-layered membrane, which also improved drug entrapment.[46] Similarly, the EE% was increased in the niosomal dosage form N2 upon increasing the concentration of cholesterol, compared to N1, resulting in higher formulation viscosity, and membrane firmness which improved the physical stability.[47] A previous research reported that optimal drug entrapment in niosomes could be attained at cholesterol: surfactant ratio 1:1.[48]

Additionally, the use of Tween 80 as a surfactant in SP2 instead of Brij in SP1 could be responsible for the smaller size of SP2, due to the reduced surface energy and water uptake of the less hydrophilic surfactant.[48] On the other hand, the smaller vesicle size of N2 relative to N1 could be attributed also to the higher concentration of cholesterol that enhanced the hydrophobicity of the bilayer of the nanovesicles resulting in a reduced surface free energy and thus decreasing the vesicular size.[38,49] Small vesicular size of topical formulations is an essential requirement to augment permeation through the skin and provide large surface area for enhanced diffusion. It is worth to note that ethanol used in the preparation of the formulations is supposed to decrease the thickness of the nanovesicular membrane, and consequently change the surface charge, reduce vesicular size, and provide more steric stabilization.[50,51] The uniform PDI values of the prepared nanovesicles indicate optimal formulation homogeneity.[52] This can be attributed to the application of the spraying technique to prepare the formulations, which was shown previously to provide homogenous distribution of the prepared nano-vesicles.[26] The enhanced diffusion of the prepared nano-vesicles through the excised rat skin compared to celecoxib suspension could be attributed to the permeation enhancement

Table 6 Percentage of Reduction in Edema Circumference

Formulation	Day 21% Inhibition	Day 23% Inhibition	Day 25% Inhibition	Day 30
Group III (diclofenac treated)	7.1 ± 1.8	15.6 ± 1.94	23.6± 2.1	42.13 ± 2.2
Group IV (celecoxib gel)	6.5 ± 2.3	17.5 ± 3.2	21.9 ± 3.6	40.25 ± 4.3
Group V (niosomal gel)	5.4 ± 1.5	25.8 ± 2.4	38.4± 2.8	64.1 ± 3.5***
Group VI (spanlastic gel)	5.8 ± 0.7	29.1 ± 1.5	48.6± 2.3	73. 5 ± 2.6***

Note: ***p<0.005.

Table 7 Mean Relative Gene Expression of TNFα, NF-kB and COX-2 in Paw Tissue of Study Groups

Groups	TNFα	NF-kB	COX-2
I (negative control)	1.0	1.0	1.0
II (arthritic positive control)	4.13 ± 0.3619	5.51 ± 0.2257	6.11 ± 0.5097
III (diclofenac treated)	2.436 ± 0.1987***	2.458 ± 0.1581***	3.792 ± 0.227***
IV (celecoxib gel)	2.354 ± 0.1194***	2.308 ± 0.1122***	3.8 ± 0.133***
V (Spanlastic gel)	1.53 ± 0.04899***	1.4 ± 0.03647***	1.94 ± 0.1015***
VI (niosomal gel)	1.95 ± 0.08695***	1.88 ± 0.08276***	2.202 ± 0.1569***

Note: ***p<0.005.

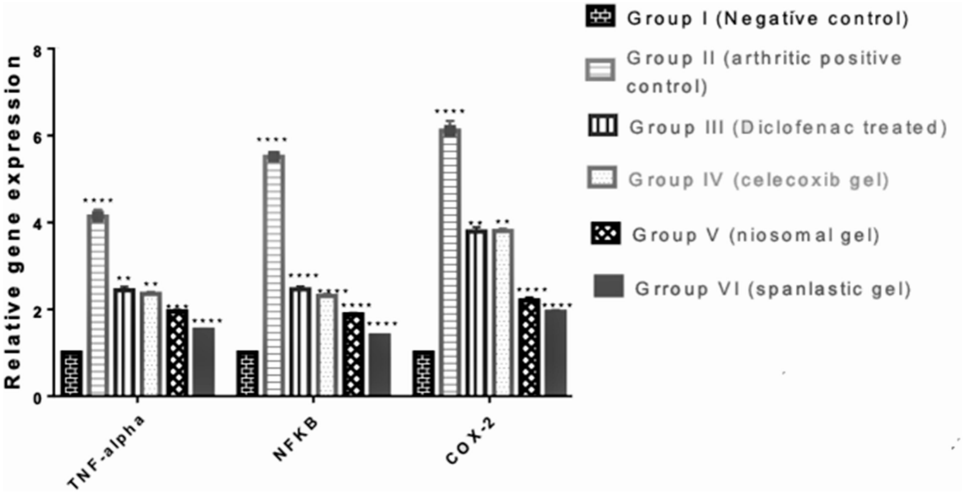

Figure 5 Relative mRNA expression of TNF-α, NFKB and COX-2 in paw tissue of Freund's complete adjuvant-induced arthritis in rats. ****p<0.0001, ***p<0.005, **p<0.01.

effect of the included non-ionic surfactants. These surfactants decrease the crystalline properties of the intracellular lipid bilayer of the skin which improves permeation.[53] The superior permeation results of SP2 could be explained on the basis that spanlastics have the ability to deliver celecoxib as a very fine colloidal dispersion with greater surface area, which minimizes the drug diffusional path length through the skin.[54] Besides, modifying of the nanovesicles with the edge activator is another factor that contributes to the improved skin diffusion as it increases spanlastic deformability and consequently augments the capacity of the vesicles to keep and bind water when applied under non-occlusive state to avoid dehydration.[42,55–57] Accordingly, spanlastics provides deep relocation to water opulent strata to guarantee appropriate hydration condition. In addition, edge activator has a high tendency for exceedingly curved framework; a characteristic that enables spanlastics to generate stress-dependent alteration of their existing assembly to overcome their movement reluctance through the restraining skin channels and hence permits reproducible drug passage.[58] The higher permeation of SP2 relative to SP1 could be attributed to the smaller vesicle size and the highly elastic and non-bulky hydrocarbon chains of Tween 80.[42]

Formulation of N2 and SP2 into gel was essential to increase the residence time on the skin after application. The obvious pseudoplastic or shear-thinning performance of the prepared gels is favorable for topical application because of the ease of spreadability.[59,60] Fitting of the permeation data to different mathematical models revealed that the Higuchi's model fits the experimental data the most, which indicates that diffusion is the possible release mechanism of celecoxib from the prepared nano-vesicles and selected gels.

In rats with Freund's Complete adjuvant-induced RA, the relative expression levels of TNF-α, NF-κB and COX-2 are higher compared to those of the non-arthritic group. The augmented TNF-α, NF-κB and COX-2 levels in the arthritic control rats were significantly reduced in the treated rats treated either with diclofenac or celecoxib formulations. NF-κB is an important transcription factor in macrophages that controls gene expression for various cytokines and plays a significant role in RA development.[61] It has been reported that NF-κB controls TNF-α expression, while, TNF-α works as an inducer of NF-κB stimulation.[60] Hence, TNF-α suppression produces an overall decrease of the pro-inflammatory cytokines that require NF-κB for their expression.[62] Moreover, prostaglandin E2 (PGE2) biosynthesis from arachidonic acid by COX-2 has an important role in rheumatoid arthritis development in the synovium.[63] Increased PGE2 intensifies vasodilation, pain, and bone and cartilage erosions.[61] Increased COX-2 levels were found in arthritic control animals with subsequent enlarged paw circumference, whereas a significant reduction was detected after treatment in a manner related to the extent of permeation of the applied COX-2 inhibitor. Indeed, the anti-inflammatory effect of the celecoxib-containing spanlastic gel formulation showed the most effective alleviation of inflammation as seen in the mean relative expression values of the studied markers compared to the arthritic control group. The study recommends the use of spanlastic gel as a novel

form for the topical delivery of celecoxib for the treatment of RA.

Conclusion

In the existing study, spanlastics and niosomes were developed as nanovesicles for the topical delivery of celecoxib to treat arthritis. Our approach was to enhance the therapeutic effect of celecoxib via enhancing the permeation of celecoxib at the inflammation site while avoiding the well-reported side effects of the drug. Celecoxib-loaded spanlastic-containing gel displayed superior results in terms of reduction of circumference of edema and suppressing the arthritis markers in Freund's complete adjuvant-induced arthritis in a rat model.

Acknowledgments

The authors acknowledge all the assistants in the Pharmaceutics and Biochemistry laboratories in Deraya university for assistance in the study.

Author Contributions

Eman Alaaeldin developed the theory, performed the computations and carried out the experiments, Heba A. Abou-Taleb performed the computations and analysed the results, Soad A. Mohamad contributed to the overall interpretation of the results, Mahmoud Elrehany and Shereen Gaber designed and performed the in vivo study and provided the relevant discussion and Heba Mansour wrote the manuscript and analysed the results. All authors contributed to data analysis, and drafting/revising the article, agreed on the journal to which the article will be submitted, gave final approval of the version to be published, and agreed to be accountable for all aspects of the work.

Disclosure

The authors report no conflicts of interest for this work.

References

1. Feng S, Zhu L, Huang Z, et al. Controlled release of optimized electroporation enhances the transdermal efficiency of sinomenine hydrochloride for treating arthritis in vitro and in clinic. *Drug Des Devel Ther*. 2017;11:1737. doi:10.2147/DDDT.S136313
2. Abu-Soud HM, Wu C, Ghosh DK, et al. Stopped-flow analysis of CO and NO binding to inducible nitric oxide synthase †. *Biochemistry*. 1998;37(11):3777–3786. doi:10.1021/bi972398q
3. Lee W-S, Lim J-H, Sung M-S, et al. Ethyl acetate fraction from Angelica sinensis inhibits IL-1β-induced rheumatoid synovial fibroblast proliferation and COX-2, PGE2, and MMPs production. *Biol Res*. 2014;47(1):41. doi:10.1186/0717-6287-47-41
4. Shimomura K, Kanamoto T, Kita K, et al. Cyclic compressive loading on 3D tissue of human synovial fibroblasts upregulates prostaglandin E2 via COX-2 production without IL-1β and TNF-α. *Bone Joint Res*. 2014;3(9):280–288. doi:10.1302/2046-3758.39.2000287
5. Lee KH, Abas F, Mohamed Alitheen, NB, et al. Chemopreventive effects of a curcumin-like diarylpentanoid [2, 6-bis (2, 5-dimethoxybenzylidene) cyclohexanone] in cellular targets of rheumatoid arthritis in vitro. *Int J Rheum Dis*. 2015;18(6):616–627. doi:10.1111/1756-185X.12341
6. Fary RE, Carroll GJ, Briffa TG, et al. The effectiveness of pulsed electrical stimulation (E-PES) in the management of osteoarthritis of the knee: a protocol for a randomised controlled trial. *BMC Musculoskelet Disord*. 2008;9(1):1–9. doi:10.1186/1471-2474-9-18
7. Bennell KL, Hunter DJ, Hinman RS. Management of osteoarthritis of the knee. *BMJ*. 2012;345:e4934. doi:10.1136/bmj.e4934
8. Iannitti T, Rosini S, Lodi D, et al. Bisphosphonates: focus on inflammation and bone loss. *Am J Ther*. 2012;19(3):228–246. doi:10.1097/MJT.0b013e318247148f
9. Iannitti T, Fistetto G, Esposito A, et al. Pulsed electromagnetic field therapy for management of osteoarthritis-related pain, stiffness and physical function: clinical experience in the elderly. *Clin Interv Aging*. 2013;8:1289. doi:10.2147/CIA.S35926
10. Kaur K, Jain S, Sapra B, et al. Niosomal gel for site-specific sustained delivery of anti-arthritic drug: in vitro-in vivo evaluation. *Curr Drug Deliv*. 2007;4(4):276–282. doi:10.2174/156720107782151250
11. Fan C, Li X, Zhou Y, et al. Enhanced topical delivery of tetrandrine by ethosomes for treatment of arthritis. *Biomed Res Int*. 2013;2013:1–13. doi:10.1155/2013/161943
12. El Menshawe SF, Nafady MM, Aboud HM, et al. Transdermal delivery of fluvastatin sodium via tailored spanlastic nanovesicles: mitigated Freund's adjuvant-induced rheumatoid arthritis in rats through suppressing p38 MAPK signaling pathway. *Drug Deliv*. 2019;26(1):1140–1154. doi:10.1080/10717544.2019.1686087
13. Moghimipour E, Salami A, Monjezi M. Formulation and evaluation of liposomes for transdermal delivery of celecoxib. *Jundishapur J Nat Pharm Prod*. 2015;10(1). doi:10.17795/jjnpp-17653
14. Mahmoud MO, Aboud HM, Hassan AH, et al. Transdermal delivery of atorvastatin calcium from novel nanovesicular systems using polyethylene glycol fatty acid esters: ameliorated effect without liver toxicity in poloxamer 407-induced hyperlipidemic rats. *J Controll Release*. 2017;254:10–22. doi:10.1016/j.jconrel.2017.03.039
15. Mostafa M, Alaaeldin E, Aly UF, et al. Optimization and characterization of thymoquinone-loaded liposomes with enhanced topical anti-inflammatory activity. *AAPS PharmSciTech*. 2018;19(8):3490–3500. doi:10.1208/s12249-018-1166-1
16. Fahmy AM, El-Setouhy DA, Habib BA, et al. Enhancement of transdermal delivery of haloperidol via spanlastic dispersions: entrapment efficiency vs. particle size. *AAPS PharmSciTech*. 2019;20(3):95. doi:10.1208/s12249-019-1306-2
17. Abdelrahman FE, Elsayed I, Gad MK, et al. Response surface optimization, ex vivo and in vivo investigation of nasal spanlastics for bioavailability enhancement and brain targeting of risperidone. *Int J Pharm*. 2017;530(1–2):1–11. doi:10.1016/j.ijpharm.2017.07.050
18. Shakeel F, Baboota S, Ahuja A, Ali J, Faisal MS, Shafiq S. Stability evaluation of celecoxib nanoemulsion containing Tween 80. *Thai J Pharm Sci*. 2008;32:4–9.
19. Dave V, Gupta A, Singh P, et al. PEGylated Lipova E120 liposomes loaded with celecoxib: in-vitro characterization and enhanced in-vivo anti-inflammatory effects in rat models. *J Biosci*. 2019;44(4):94. doi:10.1007/s12038-019-9919-x
20. Perumal V, Banerjee S, Das S, et al. Effect of liposomal celecoxib on proliferation of colon cancer cell and inhibition of DMBA-induced tumor in rat model. *Cancer Nanotechnol*. 2011;2(1–6):67–79. doi:10.1007/s12645-011-0017-5

21. Auda SH, Fathalla D, Fetih G, et al. Niosomes as transdermal drug delivery system for celecoxib: in vitro and in vivo studies. *Polym Bull*. 2016;73(5):1229–1245. doi:10.1007/s00289-015-1544-8
22. Perlstein H, Bavli Y, Turovsky T, et al. Beta-casein nanocarriers of celecoxib for improved oral bioavailability. *Eur J Nanomed*. 2014;6 (4):217–226. doi:10.1515/ejnm-2014-0025
23. Ventura C, Tommasini S, Falcone A, et al. Influence of modified cyclodextrins on solubility and percutaneous absorption of celecoxib through human skin. *Int J Pharm*. 2006;314(1):37–45. doi:10.1016/j.ijpharm.2006.02.006
24. Mokhtar M, Sammour OA, Hammad MA, et al. Effect of some formulation parameters on flurbiprofen encapsulation and release rates of niosomes prepared from proniosomes. *Int J Pharm*. 2008;361(1–2):104–111. doi:10.1016/j.ijpharm.2008.05.031
25. El-Badry M, Fetih G. Preparation, characterization and anti-inflammatory activity of celecoxib chitosan gel formulations. *J Drug Deliv Sci Technol*. 2011;21(2):201–206. doi:10.1016/S1773-2247(11)50023-1
26. Refaat H, Naguib YW, Elsayed MMA, et al. Modified spraying technique and response surface methodology for the preparation and optimization of propolis liposomes of enhanced anti-proliferative activity against human melanoma cell line A375. *Pharmaceutics*. 2019;11(11):558. doi:10.3390/pharmaceutics11110558
27. Barry BW. Novel mechanisms and devices to enable successful transdermal drug delivery. *Eur J Pharm Sci*. 2001;14(2):101–114. doi:10.1016/S0928-0987(01)00167-1
28. Qiu Y, Gao Y, Hu K, Li F. Enhancement of skin permeation of docetaxel: a novel approach combining microneedle and elastic liposomes. *J Controll Release*. 2008;129(2):144–150.
29. Bisht D, Verma D, Mirza MA, et al. Development of ethosomal gel of ranolazine for improved topical delivery: in vitro and ex vivo evaluation. *J Mol Liq*. 2017;225:475–481. doi:10.1016/j.molliq.2016.11.114
30. Patel DS, Patel SD, Kurani SP. Preparation of selective cyclooxygenase II inhibitors. Google Patents; 2003.
31. New RR Preparation of liposomes. Liposomes: a practical approach; 1990:33–104.
32. Ruozi B, Tosi G, Forni F, et al. Atomic force microscopy and photon correlation spectroscopy: two techniques for rapid characterization of liposomes. *Eur J Pharm Sci*. 2005;25(1):81–89. doi:10.1016/j.ejps.2005.01.020
33. Ruddy SB, Matuszewska BK, Grim YA, et al. Design and characterization of a surfactant-enriched tablet formulation for oral delivery of a poorly water-soluble immunosuppressive agent. *Int J Pharm*. 1999;182(2):173–186. doi:10.1016/S0378-5173(99)00056-3
34. Chen LR, Wesley JA, Bhattachar S, et al. Dissolution behavior of a poorly water soluble compound in the presence of Tween 80. *Pharm Res*. 2003;20(5):797–801. doi:10.1023/A:1023493821302
35. Ruckmani K, Sankar V. Formulation and optimization of zidovudine niosomes. *AAPS PharmSciTech*. 2010;11(3):1119–1127. doi:10.1208/s12249-010-9480-2
36. Elsayed MM, Mostafa ME, Alaaeldin E, et al. Design and characterisation of novel Sorafenib-loaded carbon nanotubes with distinct tumour-suppressive activity in hepatocellular carcinoma. *Int J Nanomedicine*. 2019;14:8445. doi:10.2147/IJN.S223920
37. Alaaeldin E, Gomaa MD, Eltewacy NK, et al. Formulation and characterization of thymoquinone bioadhesive gel for treatment of chronic gum inflammation.
38. Kumbhar D, Wavikar P, Vavia P. Niosomal gel of lornoxicam for topical delivery: in vitro assessment and pharmacodynamic activity. *AAPS PharmSciTech*. 2013;14(3):1072–1082. doi:10.1208/s12249-013-9986-5
39. He YH, Zhou J, Wang Y-S, et al. Anti-inflammatory and anti-oxidative effects of cherries on Freund's adjuvant-induced arthritis in rats. *Scand J Rheumatol*. 2006;35(5):356–358. doi:10.1080/03009740600704155
40. Dorazil-Dudzik M, Mika J, Schafer MK-H, et al. The effects of local pentoxifylline and propentofylline treatment on formalin-induced pain and tumor necrosis factor-α messenger RNA levels in the inflamed tissue of the rat paw. *Anesth Analg*. 2004;98 (6):1566–1573. doi:10.1213/01.ANE.0000113235.88534.48
41. ElMeshad AN, Mohsen AM. Enhanced corneal permeation and antimycotic activity of itraconazole against Candida albicans via a novel nanosystem vesicle. *Drug Deliv*. 2016;23(7):2115–2123. doi:10.3109/10717544.2014.942811
42. Qumbar M, Imam SS, Ali J, Ahmad J, Ali A. Formulation and optimization of lacidipine loaded niosomal gel for transdermal delivery: in-vitro characterization and in-vivo activity. *Biomed Pharmacother*. 2017;93:255–266. doi:10.1016/j.biopha.2017.06.043
43. Alharbi KS, Alruwaili NK, Imam SS, et al. Formulation of chitosan polymeric vesicles of ciprofloxacin for ocular delivery: box-behnken optimization, in vitro characterization, HET-CAM irritation, and antimicrobial assessment. *AAPS PharmSciTech*. 2020;21(5):167. doi:10.1208/s12249-020-01699-9
44. Nowroozi F, Almasi A, Javidi J, et al. Effect of surfactant type, cholesterol content and various downsizing methods on the particle size of niosomes. *Iran J Pharm Res*. 2018;17(Suppl2):1.
45. Das MK, Palei NN. Sorbitan ester niosomes for topical delivery of rofecoxib; 2011.
46. Agarwal S, Bakshi V, Vitta P, et al. Effect of cholesterol content and surfactant HLB on vesicle properties of niosomes. *Indian J Pharm Sci*. 2004;66(1):121–123.
47. Kamboj S, Saini V, Bala S. Formulation and characterization of drug loaded nonionic surfactant vesicles (niosomes) for oral bioavailability enhancement. *Sci World J*. 2014;2014:1–8. doi:10.1155/2014/959741
48. Barry JA, Gawrisch K. Direct NMR evidence for ethanol binding to the lipid-water interface of phospholipid bilayers. *Biochemistry*. 1994;33(26):8082–8088. doi:10.1021/bi00192a013
49. Cho H-J, Park JW, Yoon I-S, et al. Surface-modified solid lipid nanoparticles for oral delivery of docetaxel: enhanced intestinal absorption and lymphatic uptake. *Int J Nanomedicine*. 2014;9:495.
50. Jain S, Chaudhari BH, Swarnakar NK. Preparation and characterization of niosomal gel for iontophoresis mediated transdermal delivery of isosorbide dinitrate. *Drug Deliv Transl Res*. 2011;1(4):309–321.
51. Fahmy UA. Nanoethosomal transdermal delivery of vardenafil for treatment of erectile dysfunction: optimization, characterization, and in vivo evaluation. *Drug Des Devel Ther*. 2015;9:6129. doi:10.2147/DDDT.S94615
52. El Zaafarany GM, Awad GAS, Holayel SM, et al. Role of edge activators and surface charge in developing ultradeformable vesicles with enhanced skin delivery. *Int J Pharm*. 2010;397(1–2):164–172. doi:10.1016/j.ijpharm.2010.06.034
53. Cevc G, Blume G. Biological activity and characteristics of triamcinolone-acetonide formulated with the self-regulating drug carriers, Transfersomes®. *Biochim Biophys Acta Biomembr*. 2003;1614 (2):156–164. doi:10.1016/S0005-2736(03)00172-X
54. Hussein AK, Mansour HF. Oxiconazole nitrate solid lipid nanoparticles: formulation, in-vitro characterization and clinical assessment of an analogous loaded carbopol gel. *Drug Dev Ind Pharm*. 2020;46 (5):706–716. doi:10.1080/03639045.2020.1752707
55. Imam SS, Ahad A, Aqil M, et al. Formulation by design based risperidone nano soft lipid vesicle as a new strategy for enhanced transdermal drug delivery: in-vitro characterization, and in-vivo appraisal. *Mater Sci Eng C*. 2017;75:1198–1205. doi:10.1016/j.msec.2017.02.149
56. Imam SS, Aqil M, Akhtar M, et al. Formulation by design-based proniosome for accentuated transdermal delivery of risperidone: in vitro characterization and in vivo pharmacokinetic study. *Drug Deliv*. 2015;22(8):1059–1070. doi:10.3109/10717544.2013.870260
57. Mohanty D, Rani MJ, Haque MA, et al. Preparation and evaluation of transdermal naproxen niosomes: formulation optimization to preclinical anti-inflammatory assessment on murine model. *J Liposome Res*. 2019:1–11.

58. El-Ridy MS, Yehia SA, Mohsen AM, et al. Formulation of Niosomal gel for enhanced transdermal lornoxicam delivery: in-vitro and in-vivo evaluation. *Curr Drug Deliv*. 2018;15(1):122–133. doi:10.2174/1567201814666170224141548
59. Kim D, Shin EK, Kim YH, et al. Suppression of inflammatory responses by celastrol, a quinone methide triterpenoid isolated from Celastrus regelii. *Eur J Clin Invest*. 2009;39(9):819–827. doi:10.1111/j.1365-2362.2009.02186.x
60. Makarov SS. NF-κB in rheumatoid arthritis: a pivotal regulator of inflammation, hyperplasia, and tissue destruction. *Arthritis Res Ther*. 2001;3(4):1–7.
61. Fattahi MJ, Mirshafiey A. Prostaglandins and rheumatoid arthritis. *Arthritis*. 2012;2012:1–7. doi:10.1155/2012/239310
62. Taylor SL, Krempel RL, Schmaljohn CS. Inhibition of TNF-α-induced activation of NF-κB by hantavirus nucleocapsid proteins. *Ann N Y Acad Sci*. 2009;1171:E86–E93. doi:10.1111/j.1749-6632.2009.05049.x
63. Cheng X-L, Liu X-G, Wang Q, et al. Anti-inflammatory and anti-arthritic effects of Guge Fengtong formula: in vitro and in vivo studies. *Chin J Nat Med*. 2015;13(11):842–853. doi:10.1016/S1875-5364(15)30088-1